Rich Structural and Magnetic Chemistry of Cobalt(II) Pyrimidin-2-olate and Pyrimidin-4-olate Complexes. Synthesis, X-ray Powder Diffraction Studies, and Thermal Behavior

ARTICLE *in* CHEMISTRY OF MATERIALS · MAY 2003

Impact Factor: 8.35 · DOI: 10.1021/cm030195k

Rich Structural and Magnetic Chemistry of Cobalt(II) Pyrimidin-2-olate and Pyrimidin-4-olate Complexes. Synthesis, X-ray Powder Diffraction Studies, and Thermal Behavior

Norberto Masciocchi,*[,†] Simona Galli,[†] Angelo Sironi,[‡] Elisa Barea,[§] Jorge A. R. Navarro,*[,§] Juan M. Salas,[§] and Leandro C. Tabares[§,||]

Dipartimento di Scienze Chimiche, Fisiche e Matematiche, Università degli Studi dell'Insubria, via Valleggio 11, I-22100 Como, Italy, Dipartimento di Chimica Strutturale e Stereochimica Inorganica, Università degli Studi di Milano, via Venezian 21, I-20133 Milano, Italy, and Departamento de Química Inorgánica, Universidad de Granada, Av. Fuentenueva S/N, E-18071 Granada, Spain

Received January 30, 2003. Revised Manuscript Received March 25, 2003

Two new cobalt(II) species containing the pyrimidin-4-olate ligand (4-pymo) have been prepared and fully characterized by spectroscopic, thermal, and ab initio X-ray powder diffraction methods. The magnetic properties of both these species and $Co(2\text{-pymo})_2$, an extended cobalt(II) compound containing the pyrimidine-2-olate ligand (2-pymo), are also reported. $Co(4\text{-pymo})_2(H_2O)_4$ (**1**) [orthorhombic, *Pcab*, $a = 13.5233(4)$ Å, $b = 12.9617(3)$ Å, and $c = 6.7925(2)$ Å] consists of D_{4h} octahedral monomers, bearing axial 4-pymo ligands, interlinked by an extensive network of OH···X (X = O, N) hydrogen bonds. Upon heating, it loses water and transforms into an amorphous (above 150 °C) (**2a**) or a polycrystalline (above 320 °C) $Co(4\text{-pymo})_2$ phase (**2b**) [orthorhombic, *Imma*, $a = 6.5720(8)$ Å, $b = 6.6209(8)$ Å, and $c = 20.688(2)$ Å]. In the latter, C_{2v} pseudo-tetrahedral cobalt(II) ions are linked by 4-pymo ligands in the unusual *N*,*O*-*exo*-bidentate mode, generating 2D layers of nearly square meshes, thus significantly differing from the $Co(2\text{-pymo})_2$ analogue (**3**), in which *N*,*N*′-*exo*-bidentate bridges generate an acentric, 3D diamondoid network. The thermal dependence of the magnetic susceptibility has been studied for all the above compounds (**1**, **2a**, **2b**, and **3**) in the 2−300 K temperature range. The magnetic behavior of **1** is dominated by spin−orbit coupling of magnetically isolated octahedral Co(II) centers. The extended materials **2a** and **2b** show antiferromagnetic exchange between distorted tetrahedral metal centers, whereas **3** behaves as a spin-canted antiferromagnet, a ferromagnetic ordering taking place below a critical temperature, $T_c = 23$ K; **3** can thus be considered as a molecular magnet. Indeed, magnetic hysteresis studies on **3** at 4.8 K yield a coercitive field $H_{coer} = 3900$ G and a remnant magnetization $M_{rem} = 279$ cm^3 G mol^{-1}.

Introduction

Polymeric coordination compounds in which transition metals are bridged by polyazaheteroaromatic ligands have been found to possess interesting characteristics, such as high thermal stability[1] or magnetic,[2] sorptive,[3] luminescent,[4] nonlinear optical,[5] thermochromic,[6] and catalytic[7] properties. To provide homoleptic end members, which can be a valuable help in highlighting the origin of such properties and their possible tunability, simple transition metal pyrazolates, imidazolates, and pyrimidin-2-olates (2-pymo's in the following) have been synthesized and structurally characterized almost exclusively by X-ray diffraction from microcrystalline powders (XRPD hereafter).[8]

To extend the above study, our attention has recently turned to pyrimidin-4-olate (4-pymo), differing from 2-pymo for its oxygen position (ortho vs para with respect to N_1, this eventually lowering its symmetry, see Chart 1, where the labeling scheme adopted throughout the paper is highlighted) and, slightly, for its steric

* To whom correspondence should be addressed. Tel.: +39-031-326227. Fax: +39-031-2386119. E-mail: norberto.masciocchi@uninsubria.it.

† Università degli Studi dell'Insubria.

‡ Università degli Studi di Milano.

§ Universidad de Granada.

|| Present address: Area Biología Molecular-IBR Suipacha 531, S2002LRK Rosario, Argentina.

(1) Masciocchi, N.; Ardizzoia, G. A.; La Monica, G.; Maspero, A.; Sironi, A. *Eur. J. Inorg. Chem.* **2000**, 2507.

(2) Kahn, O.; Jay, C. *Science* **1998**, *279*, 44.

(3) Uemura, K.; Kitagawa, S.; Kondo, M.; Fukui, K.; Kitaura, R.; Chang, H. C.; Mizutani, T. *Chem. Eur. J.* **2002**, *8*, 3587.

(4) Burini, A.; Bravi, R.; Fackler, J. P. Jr.; Galassi, R.; Grant, T. A.; Omary, M. A.; Pietroni, B. R.; Staples, R. J. *Inorg. Chem.* **2000**, *39*, 3158, and references therein.

(5) Thompson, M. E.; Chiang, W. C.; Myers, L. K.; Langhoff, C. A. In *Nonlinear Optics and Materials*; Cantrell, C. D., Ed.; SPIE Proceedings: Bellingham, WA, 1991; Vol. 1497, p 423.

(6) Verelst, M.; Sommier, L.; Lecante, P. O.; Mosset, A.; Kahn, O. *Chem. Mater.* **1998**, *10*, 980.

(7) Fujita, M.; Kwon, Y. J.; Washizu, S.; Ogura, K. *J. Am. Chem. Soc.* **1994**, *116*, 1151.

(8) Masciocchi, N.; Ardizzoia, G. A.; Brenna, S.; La Monica, G.; Maspero, A.; Galli, S.; Sironi, A. *Inorg. Chem.* **2002**, *41*, 6080, and references therein.

10.1021/cm030195k CCC: $25.00
Published on Web 05/06/2003

Chart 1

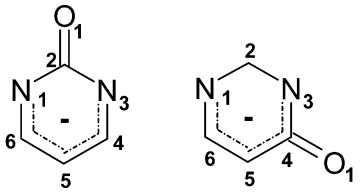

and electronic features, thus potentially offering a wider coordination versatility. A paper dealing with the reversible sorption properties of $Cu(4\text{-pymo})_2$ has recently appeared.[9] In the present contribution, we report on the $Co(4\text{-pymo})_2$ derivative and its hydrated precursor, $Co(4\text{-pymo})_2(H_2O)_4$, highlighting their magnetic features and crystal chemistry, with reference to those of the thermally robust $Co(2\text{-pymo})_2$ polymer.[1] Again, we resort to unconventional ab initio XRPD methods[10] for the full structural characterization of microcrystalline species not affording single crystals of size and quality suitable for a standard single-crystal diffraction analysis. The results obtained show the wide effect of the exocyclic oxygen position on both the structural and the magneto-chemistry of the examined compounds.

Experimental Section

General Methods. 4-Hydroxypyrimidine (4-Hpymo, from Aldrich Chemical Co.) and the other chemical reagents and solvents were acquired from available commercial sources and used as received. $Co(2\text{-pymo})_2$ was prepared as previously reported.[1] IR absorption bands were measured by a Midac FT-IR on KBr pellets. Electronic spectra of solid samples were carried out on a Varian Cary UV−vis−NIR spectrophotometer (Instrumentation Center of the University of Granada). Thermogravimetric and differential calorimetric analyses were performed, under dinitrogen or air atmospheres, on Perkin-Elmer TGA7/DSC7 (University of Milan) or Shimadzu-TGA-50H/DSC (Instrumentation Center of the University of Granada) equipment, at heating rates of 10 or 20 °C min^{-1}. Magnetic susceptibility measurements were performed on polycrystalline samples with a Quantum Design MPMS-2SQUID magnetometer operating in the temperature range 2−300 K and at magnetic field strength values between 0.5 and 10 kG.

Preparation of $Co(4\text{-pymo})_2(H_2O)_4$ (1). An aqueous solution (40 mL) containing 4-Hpymo (4 mmol) and NaOH (4 mmol) was added dropwise into an aqueous solution of $Co(AcO)_2{\cdot}6H_2O$ (2 mmol). The resulting suspension was stirred at room temperature for 2 h, affording a pale pink microcrystalline material, which was washed with ethanol and diethyl ether and dried in air. Yield 85%. Anal. Calcd for $C_8H_{14}CoN_4O_6$: C, 29.92; H, 4.39; N, 17.45. Found: C, 29.9; H, 4.6; N, 17.4. IR (selected bands in cm^{-1}): 1603 vs, 1518 s, 1477 s, 1416 vs, 1329 s, 1020 s, 837 br, s. UV−vis (nm): 205 vs, 230 vs, 500 m, 1150 br.

Preparation of $Co(4\text{-pymo})_2$, 2a (Amorphous Phase), and 2b (Crystalline Phase). Two hundred milligrams of **1** was heated at 130 °C for 24 h, affording a purple amorphous phase of formula $Co(4\text{-pymo})_2$ (**2a**). **2a** could be alternatively obtained by refluxing **1** for 2 h in dry DMF. Anal. Calcd for $C_8H_6CoN_4O_2$: C, 38.57; H, 2.43; N, 22.49. Found: C, 37.9; H, 2.5; N, 22.2. IR (selected bands in cm^{-1}): 1611 vs, 1539 s, 1487 s, 1425 s, 1332 m, 1020 m, 839 m. UV−vis (nm): 215 vs, 280 vs, 550 s, 1200 s, br. Further heating of 30 mg of **2a** under dinitrogen at a heating rate of 10 °C min^{-1} up to 320 °C afforded a purple microcrystalline material (**2b**) with no change in its analytical composition. Anal. Calcd for $C_8H_6CoN_4O_2$: C, 38.57; H, 2.43; N, 22.49. Found: C, 37.9; H, 2.4; N, 22.1. IR (selected bands in cm^{-1}): 1609 vs, 1539 s, 1489 s, 1418 s, 1327 m, 1015 m, 841 m. UV−vis (nm): 215 vs, 280 vs, 525 s, 1260 s, br.

X-ray Powder Diffraction Analysis of $Co(4\text{-pymo})_2(H_2O)_4$, 1, and $Co(4\text{-pymo})_2$, 2b. The powders were gently ground in an agate mortar and then cautiously deposited in the hollow of an aluminum holder equipped with a zero background plate (supplied by *The Gem Dugout*, State College, PA). Diffraction data (Cu Kα, $\lambda = 1.5418$ Å) were collected on a θ:θ Bruker AXS D8 diffractometer equipped with primary and secondary Soller slits (2.3°), divergence, antiscatter, and receiving slits (0.5°, 0.5°, and 0.2 mm, respectively), secondary beam curved graphite monochromator, Na(Tl)I scintillation detector, and pulse height amplifier discrimination. A generator was operated at 40 kV and 40 mA. Nominal resolution for the present setup is 0.07° 2θ (fwhm of the α_1 component) as measured from the Si(111) peak at 28.44° (2θ). Long step scans with $\Delta 2\theta = 0.02°$ were performed in the ranges $5° < 2\theta < 105°$ with $t = 30$ s/step.

For both compounds, indexing was obtained with TREOR90[11] [**1**: orthorhombic, $a = 13.51$, $b = 12.95$, $c = 6.79$ Å, M(21)[12] = 24, F(21)[13] = 39(0.009, 58); **2b**: tetragonal, $a = 6.59$, $c = 20.73$ Å, M(10) = 32, F(10) = 17(0.013, 46)]. Systematic absences indicated *Pcab* and $I4_1/amd$, respectively, as the probable space groups for **1** and **2b**. However, an accurate visual inspection of the XRPD pattern of **2b** allowed the discovery of the *highly reproducible* splitting ($\Delta 2\theta = 0.18°$) of the (0 2 0) peak (see inset in Figure 1b) as well as the high-angle broadening of some other peaks [see, for example, the (0 2 2) and (2 0 2) cluster in the inset in Figure 1b], thus indicating *orthorhombic*, rather than *tetragonal*, symmetry, with *slightly* different *a* and *b* cell parameters. Systematic absences were reconsidered in light of this observation and a body-centered *Imma* cell (a proper subgroup of $I4_1/amd$) was subsequently adopted. Note that the above splitting, though minimal, is the most evident trace of the orthorhombic nature of **2b**. Actually, as a consequence of the strict similarity between *a* and *b*, the *hkl* and *khl* Bragg peaks are almost completely superimposed: due to the large peak widths and the anisotropic peak shape broadening affecting the collected data (later interpreted as deriving from a highly strained sample), splitting of further peaks, allowing recognition of neighboring *resolved* maxima, could not be detected. For both **1** and **2b**, space group choices were confirmed by successful solution and refinement.[14] Whole profile structure solutions using simulated annealing[15] were performed with the TOPAS V2.0 suite of programs.[16] 4-pymo ligands were treated as rigid bodies, assigning to them average literature bond distances and angles (C−C and C−N distances = 1.40 Å; C−O distance = 1.25 Å; C−H distances = 0.95 Å; ring bond angles = 120.0°). In the hydrated species, **1**, even the crystallographically independent $Co(O_w)_2$ moiety (O_w = coordinated water oxygens) was treated as a rigid body (Co−O_w 2.10 Å, O_w−Co−O_w 90.0°).

(9) Barea, E.; Navarro, J. A. R.; Salas, J. M.; Masciocchi, N.; Galli, S.; Sironi, A. *Polyhedron* **2003**, in press.
(10) Masciocchi, N.; Sironi, A. *J. Chem. Soc., Dalton Trans.* **1997**, 4643.
(11) Werner, P. E.; Eriksson, L.; Westdahl, M. *J. Appl. Crystallogr.* **1985**, *18*, 367.
(12) De Wolff, P. M. *J. Appl. Crystallogr.* **1968**, *1*, 108.
(13) Smith, G. S.; Snyder, R. L. *J. Appl. Crystallogr.* **1979**, *12*, 60.
(14) In search of a crystallochemical explanation of the observed orthorhombic character, we also tested the two acentric *I*2*mb* and *Im*2*a* space groups (two proper subgroups of *Imma*). Indeed, in these space groups, the ligands are ordered along one axis (**a** or **b**) and disordered along the other one (**b** or **a**), respectively, thus differentiating the two directions. Unfortunately, the resulting models, obtained with parallel refinements, did not improve the agreement factors and were therefore discarded. Similarly, on lowering the symmetry down to the monoclinic $I\bar{1}12/b$ (disordered structure) or *I*11*b* (ordered) as well as to the triclinic $I\bar{1}$ (ordered) space groups, no better agreement was ever observed. Thus, we still have no structural explanation for the existence of an orthorhombic, rather than a tetragonal, unit cell.
(15) Coelho, A. A. *J. Appl. Crystallogr.* **2000**, *33*, 899.
(16) Bruker AXS. Topas V2.0: General profile and structure analysis software for powder diffraction data; Karlsruhe, Germany, 2000.

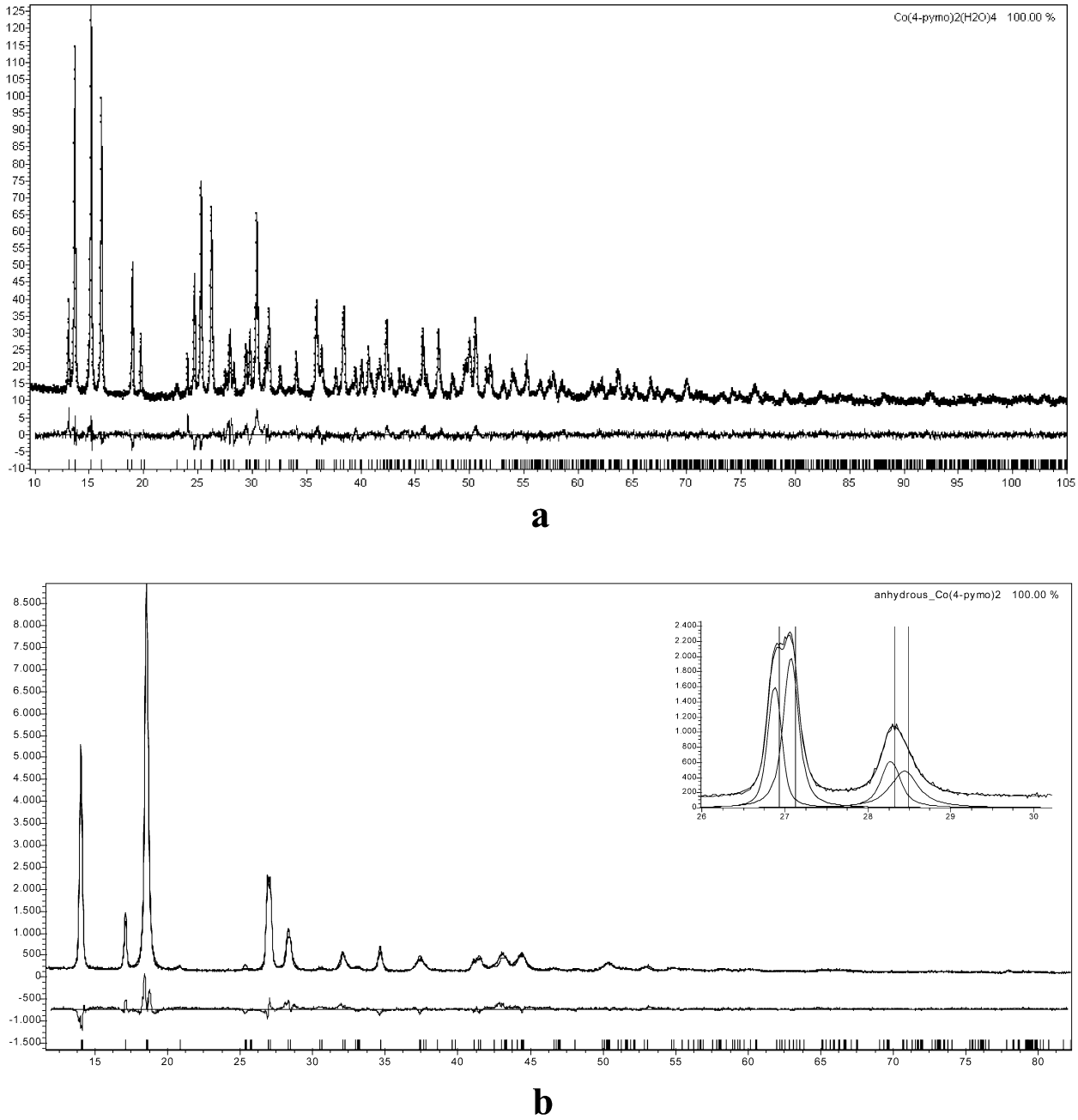

Figure 1. Final Rietveld refinement plots for $Co(4\text{-pymo})_2(H_2O)_4$ (a) and $Co(4\text{-pymo})_2$ (b), with difference plots and peak markers. In the inset of part b, the splitting of the tetragonal (0 2 0) and (0 2 2) Bragg peaks into the orthorhombic ones and the (0 2 2)−(2 0 2) cluster are magnified (see the Experimental Section for further details).

For **2b**, convergence to a chemically significant model was obtained also by imposing soft restraints on the Co−$O_{1a,b}$, 1,3-Co···$C_{2a,b}$, and 1,3-Co···$C_{6a,b}$ distances, the latter two implying a Co−N vector bisecting the C−N−C angle. The final refinements were performed, using TOPAS, by the Rietveld method, maintaining the rigid bodies and soft restraints quoted above (statistically significant standard deviations for fractional atomic coordinates are thus not available). Peak shapes were described by the fundamental parameters approach.[17] Experimental background was fit by a polynomial description. Systematic errors were modeled with sample-displacement angular shifts, preferred orientation corrections in the March-Dollase formulation[18] (with the [001] pole in both cases) and, for **2b**, anisotropic peak shape broadening (fourth-order spherical harmonics),[17] since 00*l* peaks are markedly narrower than those of the *hk*0 class. Co atoms were given a refinable, isotropic displacement parameter (B_{Co}), while lighter atoms were assigned a common $B = B_{Co} + 2.0$ Å^2 value. Scattering factors, corrected for real and imaginary anomalous dispersion terms, were taken from the internal library of TOPAS. The data below 10° (**1**) or 12° (**2b**) (2θ) have been discarded in the final refinements since they do not contain peaks of appreciable intensities. Final R_p, R_{wp}, R_B, and χ^2 agreement factors, together with details on the data collections and analyses for **1** and **2b**, can be found in Table 1. Figure 1a,b shows the final Rietveld refinement plots. Relevant structural parameters can be found throughout the text or in the figures' captions. Final fractional coordinates[19] are supplied as Supporting Information. Crystallographic data (excluding structure factors) for the two structures reported in this paper have been deposited with the Cambridge Crystallographic Data

(17) Cheary, R. W.; Coelho, A. A. *J. Appl. Crystallogr.* **1992**, *25*, 109.

(18) March, A. *Z. Kristallogr.* **1932**, *81*, 285. Dollase, W. A. *J. Appl. Crystallogr.* **1987**, *19*, 267.

Table 1. Summary of Crystal Data and Data Analysis Parameters for 1 and 2b[a]

compound	**1**	**2b**
method	XRPD	XRPD
formula	$C_8H_{14}CoN_4O_6$	$C_8H_6CoN_4O_2$
fw, g mol^{-1}	321.18	249.12
system	orthorhombic	orthorhombic
space group	*Pcab*	*Imma*
a, Å	13.5233(4)	6.5720(8)
b, Å	12.9617(3)	6.6209(8)
c, Å	6.7925(2)	20.688(2)
Z	4	4
V, Å^3	1190.6(1)	900.2(2)
ρ_{calc}, g cm^{-3}	1.792	1.839
F(000)	660	500
μ(Cu Kα), cm^{-1}	116.4	148.6
diffractometer	Bruker AXS D8	Bruker AXS D8
T, K	298(2)	298(2)
2θ range, deg	10−105	12−82
N_{data}	4750	3500
N_{obs}	676	187
R_p, R_{wp}	0.089, 0.116	0.091, 0.111
R_B	0.032	0.081
χ^2	1.84	1.89

[a] $R_p = \Sigma_i |y_{i,o} - y_{i,c}|/\Sigma_i |y_{i,o}|$; $R_{wp} = [\Sigma_i w_i(y_{i,o} - y_{i,c})^2/\Sigma_i w_i(y_{i,o})^2]^{1/2}$; $R_B = \Sigma_n|I_{n,o} - I_{n,c}|/\Sigma_n I_{n,o}$; $\chi^2 = \Sigma_i w_i(y_{i,o} - y_{i,c})^2/(N_{data} - N_{par})$, where $y_{i,o}$ and $y_{i,c}$ are the observed and calculated intensities at point *i* of the profile, respectively, while $I_{n,o}$ and $I_{n,c}$ are the observed and calculated intensities for the *n*th Bragg reflection; N_{data} is the number of observed data points, N_{obs} is that of the theoretical peaks in the considered range, and N_{par} is that of the refined parameters. Statistical weights w_i are normally taken as $1/y_{i,o}$.

Centre as supplementary publication Nos. CCDC 201589 (**1**) and 201590 (**2b**). Copies of the data can be obtained free of charge on application to CCDC, 12 Union Road, Cambridge CB2 1EZ, UK [fax: (+44)1223 336−033; e-mail: deposit@ccdc.cam.ac.uk].

Results and Discussion

Synthesis and Spectroscopy. Reaction of 4-pymo with cobalt(II) salts in aqueous solution afforded a poorly soluble microcrystalline material (**1**) with formula $Co(4\text{-pymo})_2(H_2O)_4$ and pale pink color typical of octahedral N_2O_4 cobalt(II) chromophores. Thermal treatment of **1** up to 150 °C results, concomitantly with dehydration, in a pronounced color change to deep purple, indicative of a modification in coordination geometry about the cobalt(II) centers.[20] The resulting dehydrated species (**2a**) is amorphous below 320 °C, the temperature at which it becomes crystalline. IR spectra substantiate the changes taking place on passing from **1** to **2**. The most significant ones are the shifts, to higher frequency, of the absorption bands corresponding to the pyrimidine ring vibration modes. This observation suggests a larger charge localization, as could result from O_1 involvement in metal coordination. The hypothesis of a coordinating O_1 is strengthened by the fact that ν(CO) is found to occur at lower frequencies in **2a,b** (∼1610 cm^{-1}) than in $Cu(4\text{-pymo})_2$ (1635 cm^{-1}), where 4-pymo acts in the *N,N′-exo*-bidentate mode.[9] Sample crystallinity is responsible for the sharpening of the absorption bands in **2b** compared to amorphous **2a**. Thermal treatment of **1** produces pronounced changes even on the electronic spectra. Actually, crystal d−d absorption bands are shifted to lower frequencies, with a simultaneous rise in their intensity, which is typical of a change from octahedral (forbidden transitions) to tetrahedral metal centers (allowed transitions).[20] In addition, we observe a broadening and a shifting to lower energy of a charge-transfer band [from 230 nm (**1**) to 280 nm (**2a** and **2b**)], which is indicative of the formation of an extended material.[9] The lower energy bands (d−d transitions) of the UV−vis spectra of **2a** and **2b** are very similar in form and energy, which agrees with their analogous nature.

Crystal Structure of $Co(4\text{-pymo})_2(H_2O)_4$. The $Co(4\text{-pymo})_2(H_2O)_4$ species, **1**, contains mononuclear complexes (of idealized D_{4h} symmetry) based upon *all-trans*-octahedral $Co(N_1)_2(O_w)_4$ units (N_1 = coordinated 4-pymo nitrogens; O_w = coordinated water oxygens), in which the cobalt(II) ions, lying on crystallographic inversion centers ("a" Wyckoff position), are bound to two, N_1-monodentate 4-pymo ligands and four water molecules (Figure 2a). Though mononuclear, molecules of **1** are interconnected by an extended network of intermolecular hydrogen bonds: water oxygen atoms [O_2 and O_3] interact with the "swinging" ends of the 4-pymo ligands via the noncoordinating nitrogen [N_3; $O_3\cdots N_3$ = 2.736 Å] and oxygen [O_1; $O_3\cdots O_1$ = 2.730 Å; $O_2\cdots O_1$ = 2.812 Å; $O_2\cdots O_{1'}$ = 2.844 Å] (Figure 2b). Incidentally, the former intermolecular contact helped in the unambiguous identification of the position for N_3 and in discarding the hypothesis of a disordered 4-pymo fragment. It is also worth noting that the (crystallographically unique) M−N bond distance, unconstrained during the final refinement process, reaches a value (2.159 Å) in good agreement with those of octahedral $Co(N)_2(H_2O)_4$ fragments retrieved from the CSD.

Taking into account the extensive network generated by four crystallographically independent hydrogen bonds, we can further describe species **1** as a three-dimensional polymer built upon noncovalent, highly electrostatic interactions. Accordingly, we can attribute its sudden precipitation from aqueous media (as very intractable powders) to (i) the presence of highly stabilized O_1's (formally bearing a negative charge), which interact, through three H-bonds, with neighboring O_w atoms, thus showing an overall tetrahedral coordination and (ii) the concomitant realization of the maximum possible amount of (linear) hydrogen bonds for both O_w and N_3 (two *per* O_w, one *per* N_3).

From the drawing shown in Figure 2b, one can easily detect the presence of $\pi-\pi$ stacked aromatic rings, whose centers of mass are separated by only 3.40 Å (*c*/2). Their *quasi*-eclipsed nature, in conjunction with such short ring separation, may suggest slightly repulsive $\pi-\pi$ interactions, which are, however, overwhelmed by many H-bond contacts and, possibly, by dipolar interactions between adjacent 4-pymo ligands. That weakly repulsive interactions are indeed at work is also manifested by the XRPD observation of a [001] preferred orientation pole, which clearly indicates easy cleavage or poor(er) crystal growth in the *c* direction.

A parallelism can be drawn between **1** and the recently reported $Cu(4\text{-pymo})_2(NH_3)_2(H_2O)_2$ species.[9] The substitution of two NH_3 for two H_2O ligands and the presence of a Jahn−Teller elongated, distorted

(19) The reader may find it useful to draw an ordered crystal structure from the deposited coordinates by using the nonstandard space groups *I*11*b* or *I*1, differing in the relative stacking (along **c**) of *ordered* square-meshes-based layers.

(20) Beavais, L. G.; Shores, M. P.; Long, J. R. *J. Am. Chem. Soc.* **2000**, *122*, 2763.

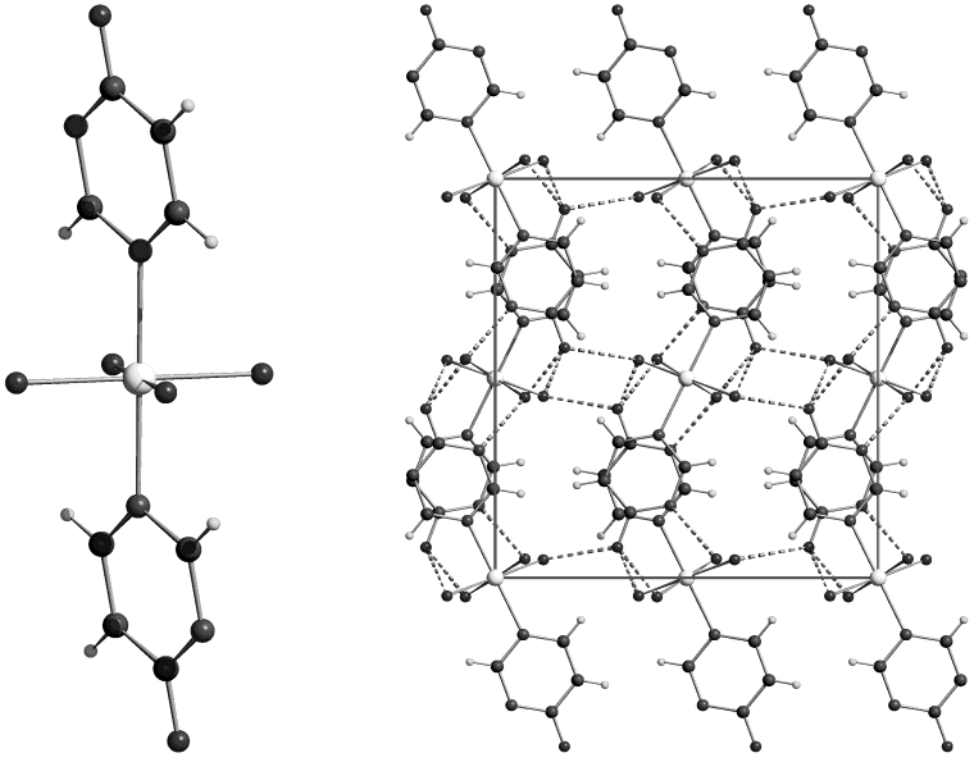

Figure 2. Schematic drawing of the $Co(4\text{-pymo})_2(H_2O)_4$ molecule (a) and its crystal packing viewed down [001] (b), highlighting the intermolecular H-bonds (fragmented lines). Cobalt atoms, large spheres in light gray. Carbon, nitrogen, and oxygen atoms, medium spheres in gray. Hydrogen atoms, small spheres in light gray.

octahedral Cu chromophore inevitably imply a lowering of symmetry, which eventually results in the monoclinic crystallographic class of the copper species vs the orthorhombic one of **1**. Actually, the monoclinic cell of the $Cu(4\text{-pymo})_2(NH_3)_2(H_2O)_2$ complex[9] ($7.189 \times 13.833 \times 6.954$ Å, $\beta = 116.23°$) can be properly described, after a rational transformation, as a pseudo-orthorhombic one ($7.473 \times 13.833 \times 12.010$ Å, $\beta = 92.12°$) with cell edges comparable to those of **1**; such transformation goes well beyond the lattice metrics, but nearly applies to all fractional atomic coordinates.

Thermal Behavior. The thermal stability of **1** was proved by thermogravimetric and differential scanning calorimetric analyses. The results indicate that the four coordinated water molecules are released, by 150 °C, in a single endothermic event ($\Delta H = 272$ kJ mol^{-1} approximately), affording the purple anhydrous and amorphous (XRPD evidence) species **2a**. Further heating beyond 320 °C promotes recrystallization of the amorphous powders into polycrystalline ones, **2b**, with an exothermic process involving ≈29 kJ mol^{-1}. Decomposition of **2b** takes place at ≈470 °C. Thus, quite like the previously reported $Co(2\text{-pymo})_2$ ($T_{dec} = 560$ °C),[10] also $Co(4\text{-pymo})_2$ may be classified as a thermally robust material. It is worth recalling that similar thermal behavior (loss of water in a one-step process to afford the anhydrous amorphous phase, later annealed to the polycrystalline one by further heating) has been previously observed for $[Ni(2\text{-pymo})_2(H_2O)_2]\cdot 0.5(H_2O)$.[10]

Crystal Structure of $Co(4\text{-pymo})_2$. This orthorhombic species contains pseudo-tetrahedral CoN_2O_2 chromophores of C_{2v} symmetry which are, however, disordered about a *mm2* crystallographic site ("e" Wyckoff position). Two crystallographically independent 4-pymo ligands bridge [in the unusual μ_2,(η^1-N_1,η^1-O_1)-*exo*-bidentate mode] cobalt ions 6.572 (along **a**) and 6.621 (along **b**) Å apart and are disordered about a crystallographic mirror plane at $y = 0.25$ and $x = 0.50$, respectively. Cobalt ions and 4-pymo ligands are organized in 2D arrays of nearly square meshes (see Figure 3, which also contains some chemically relevant bond distances and angles), stacking in a staggered fashion along **c** (omitted in Figure 3 for the sake of simplicity). Thus, even in this case, the experimental preferred orientation pole determined by diffraction methods, [001], can be easily interpreted on a structural basis.

The observed disorder is far from being random but, due to local steric requirements, must be conditioned. In particular, the ligand orientation along each $(Co\text{-}4\text{-pymo})_n$ row (running parallel to **a** or **b**) must be ordered with *all* ligands in the head-to-tail disposition. However, no correlation is expected among neither parallel nor perpendicular rows. No matter which relative orientation of these polar rows occurs, *all* cobalt atoms share the above-described local stereochemistry. The XRPD data give us further information on the relative orientation and size of such domains: the best fitting of the XRPD pattern of **2b** by the LeBail method was obtained upon inclusion of tan θ dependent Lorentzian fwhm's [giving a microstrain of 8.9×10^{-3}, in fair agreement with the $2(a - b)/(a + b)$ value of 7.4×10^{-3} computed from the refined lattice parameters]; thus, due to the mutual exchange of the slightly different *a* and *b* values, a strained sample in the **ab** plane can be envisaged. If,

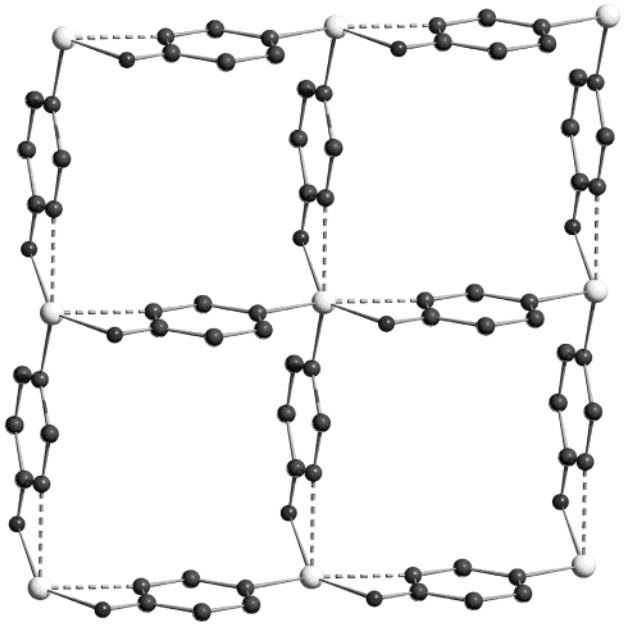

Figure 3. Partial drawing of the 2D network in Co(4-pymo)$_2$. Crystal disorder of the 4-pymo moiety and hydrogen atoms have been omitted for clarity purposes. Cobalt atoms in light gray. Carbon, nitrogen, and oxygen atoms in gray. Chemically relevant bond distances (Å) and angles (deg) are as follows: Co−N_{1a}, 2.042; Co−N_{1b}, 2.040; Co−O_{1a}, 2.200; Co−O_{1b}, 2.204; N_{1a}−Co−O_{1b}, 108.1; N_{1b}−Co−O_{1a}, 108.2; N_{1a}−Co−$O_{1a'}$, 92.4; N_{1b}−Co−$O_{1b'}$, 93.7; Co···Co, 6.572 and 6.621; Co···N_{3a}, 2.280; Co···N_{3b}, 2.329.

instead, such a broadening is attributed to size effects [with $(\cos\theta)^{-1}$ functional dependence], domains of about 600 Å are found. No matter which description is actually true, the overall microstucture of this sample can be described by a *quasi*-periodic tiling in **ab**, with local orthorhombic ($a \neq b$) symmetry, but misorientation of the domains at a slightly larger (mesoscopic) scale.

Overall, the **1** → **2b** transformation is accompanied by the following: (i) Complete loss of water molecules. (ii) Change of metal stereochemistry (from octahedral, where the metals are bound to two different 4-pymo ligands only, into pseudo-tetrahedral geometry, where metals are bound to four different 4-pymo ligands); it is worth noting, in this respect, the presence of ancillary Co···N contacts (Co···N_{3a} = 2.280 and Co···N_{3b} 2.329 Å) making each metal atom nearly six-coordinated (see Figure **3**). (iii) Change of the 4-pymo coordination mode ($\mu_1 \rightarrow \mu_2$).

The **2b** body-centered orthorhombic cell parameters (and those of the "original" tetragonal lattice) are comparable to those of the Co(2-pymo)$_2$ analogue.[1] The latter, indeed, crystallizes in the tetragonal *I*42*c* space group and is characterized by a 3D noninterpenetrated diamondoid network in which metals are tetrahedrally coordinated and 2-pymo ligands, acting in the *N*,*N*′-*exo*-bidentate fashion, are *ordered*. It is surprising that species **2b** and the Co(2-pymo)$_2$ analogue are *not* isostructural, particularly after it has been shown that the (highly porous) copper derivatives Cu(2-pymo)$_2$[21] and Cu(4-pymo)$_2$[9] are strictly isomorphous (yet, owing to the different position of the exocyclic oxygen atoms, possess

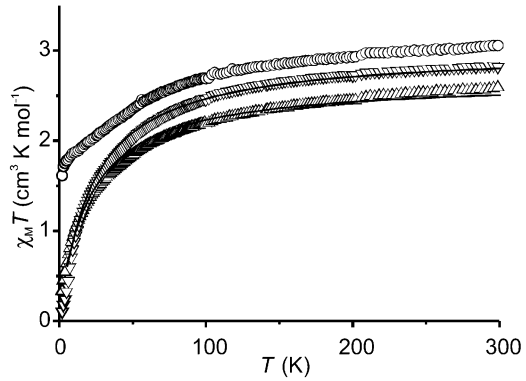

Figure 4. Field-cooled $\chi_m T$ values for **1** (○) and **2a** (Δ) and **2b** (▽) in the 2−300 K temperature range and at a field strength of 10 kG. Solid lines represent calculated values using eq 1.

relatively different sorption properties). Incidentally, eclipsed 2D arrays of [M(2-pymo)$_2$]$_4$ squares (showing *N*,*N*′-coordinated ligands) have been previously found within the tetragonal lattice of [Ni(2-pymo)$_2$(H$_2$O)$_2$]·0.5(H$_2$O),[10] with octahedral metal centers 6.327 Å apart. At variance with **2b**, in [Ni(2-pymo)$_2$(H$_2$O)$_2$]·0.5(H$_2$O), eclipsing of square grids of nominal Ni(2-pymo)$_2$ composition implies formation of channels running parallel to **c**, in which (uncoordinated) water molecules are hosted.

Magnetic Characterization. The magnetic behavior $\chi_M T$ (χ_M = molar susceptibility per cobalt atom) of **1**, **2a**, and **2b** is shown in Figure 4. $\chi_M T$ decreases in all cases upon cooling.[22]

In **1** this observation can be attributed to spin−orbit coupling of magnetically isolated octahedral cobalt(II) centers, whereas in **2a** and **2b** it should be related to antiferromagnetic exchange taking place between distorted tetrahedral metal centers, transmitted through pyrimidine-4-olate bridges. Indeed, the magnetic behavior of **2** materials can be conveniently described by eq 1 [in which the spin Hamiltonian is defined as $H = \Sigma J Si \cdot Sj$,[23] $\theta = kT/JS(S+1)$, g is the Landé g factor, μ_B is the Bohr magneton, N is the number of spins in the lattice, and the C_n coefficients have been taken from ref 23], which is adequate to describe the high temperature dependence of the magnetic susceptibility on a 2D Heisenberg quadratic-layer antiferromagnet.

$$\chi = \frac{Ng^2\mu_B{}^2}{J\left(3\theta + \sum_{n=1}^{\infty} \frac{C_n}{\theta^{n-1}}\right)} \qquad (1)$$

Fitting the data to eq 1, g values of 2.368(3) and 2.35(1) and J exchange values of −1.73(1) and −1.73(2) cm^{-1} are obtained, respectively, for **2a** and **2b**. The low absolute value of J in **2a,b** can be related to the length of the *N*,*O*-4-pymo bridges between adjacent cobalt(II) centers. The relatively high value of g might be related to the residual Co−N_3 interactions which result in a

(21) Tabares, L. C.; Navarro, J. A. R.; Salas, J. M. *J. Am. Chem. Soc.* **2001**, *123*, 383.

(22) Magnetic measurements performed on **2a** and **2b** as a function of the applied fields (500 and 10000 G) do not have any effect on the thermal behavior of their susceptibility.

(23) (a) Lines, M. E. *J. Phys. Chem. Solids* **1970**, *31*, 101. (b) Rushbrooke, G. S.; Wood, P. J. *Mol. Phys.* **1958**, *1*, 257.

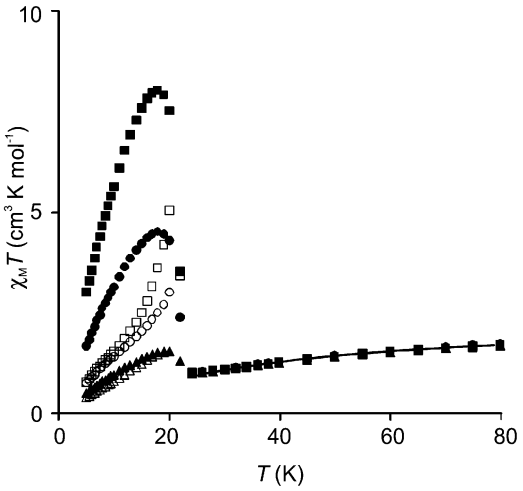

Figure 5. $\chi_m T$ values for **3** at different applied magnetic fields (0.5 kG, □; 1 kG, ○; 5 kG, △) in the 2−80 K temperature range. Field-cooled and zero-field-cooled $\chi_m T$ values are respectively presented as full and open symbols. The solid line represents calculated values using eq 1.

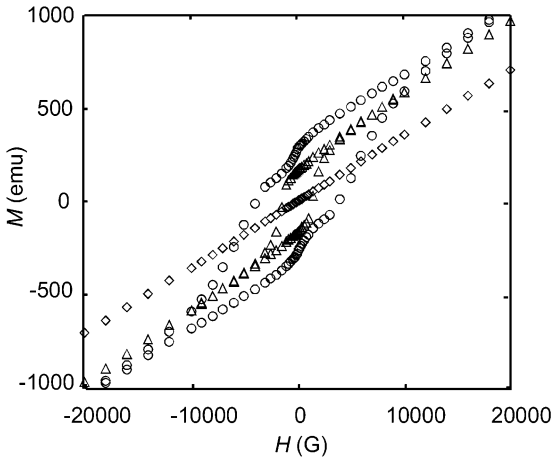

Figure 6. Magnetic hysteresis loops for **3** at 5 K (○), 20 K (△), and 30 K (◊).

distorted pseudo-octahedral geometry about the metal centers that may be responsible for some spin−orbital coupling and the overall imperfect fitting of the data to eq 1. In addition, the similarity of fitting values found for **2a** and **2b** gives further proof of their related nature.

3 shows more complex magnetic behavior. In this case, $\chi_M T$ steadily decreases upon cooling until $T_c = 23$ K. At lower temperatures, $\chi_M T$ increases, reaching a maximum around 20 K (Figure 5). The high-temperature behavior of the magnetic susceptibility is consistent with the presence of an antiferromagnetic exchange taking place between cobalt(II) centers, transmitted through the *N*,*N*′-2-pymo bridges. Fitting the data to eq 1 gives a *g* value of 2.202(5) and an exchange value, *J*, of −3.51(3) cm^{-1}. Although high, the *g* value is much lower than the one found for **2a,b**, indicating that the theoretical model behind eq 1 is appropriate to describe the high-temperature magnetic behavior of **3**.[24] The studies carried out on **3** at different field strengths clearly show that below the critical temperature, T_c, its magnetic behavior is highly dependent on the applied field. This result agrees with a spin-canted antiferromagnetic behavior,[25] a ferromagnetic ordering taking place below 23 K. Moreover, cooling the sample in a zero-field condition and rewarming it in the presence of a field, we observe that the zero-field-cooled $\chi_M T$ curve reaches a maximum just below 23 K, this being in agreement with a magnetically ordered state below this temperature. Magnetic hysteresis studies are also typical of a ferromagnetic ordering below the critical temperature (Figure 6): magnetic hysteresis measurements carried out on **3** at 4.8 K yield a coercitive field $H_{coer} =$ 3900 G and a remnant magnetization $M_{rem} = 279$ cm^3 G mol^{-1}. The spin-canted nature of **3**, rather than regular ferromagnetic behavior, is supported by the fact that the highest magnetization obtained at 4.8 K and at an applied field of 70000 G is 2903 cm^3 K mol^{-1}, which is significantly lower than the theoretical saturation value of 22300 cm^3 K mol^{-1}.[26]

The peculiar magnetic behavior of **3** can be related to the synergistic effects exerted by the electronic nature of pyrimidine-2-olate bridges, the acentric crystal structure of [Co(2-pymo)$_2$], and the magnetic anisotropy of cobalt(II) centers. In this respect, it has been observed that spin polarization effects on an aromatic ring is an efficient means to determine the magnetic interaction transmitted between species with unpaired electrons.[27] Indeed, unsubstituted pyrimidine bridging ligands have been shown to efficiently transmit a ferromagnetic interaction on a cobalt(II) layered compound.[28] Previous examples of pyrimidin-2-olate[21,29] and pyrimidine-4-olate[9] copper(II) extended systems show, however, antiferromagnetic interactions to dominate the overall magnetic behavior. Therefore, the acentric nature of **3** permits highlighting the spin-polarization effect exerted by the *N*,*N*′-*exo*-bidentate-pyrimidine-2-olate bridges, which leads to the observed 3D magnetic ordering at low temperatures.

Conclusions

Although pyrimidine-4-olate and pyrimidine-2-olate ligands are apparently very simple and closely related to each other, they are responsible for a great versatility in molecular architectures. Actually, as shown in this report, the less symmetric pyrimidine-4-olate can act either as an *N*-monodentate ligand, as in **1**, or as a *N*,*O*-*exo*-bidentate bridge, as in the extended material **2**, obtained from the former by thermal treatment. On the other hand, the more symmetric pyrimidine-2-olate ligand typically prefers the *N*,*N*′-*exo*-bidentate bridging mode, as in the extended material **3**. The different structural features resulting from the quoted coordination modes are responsible for the wide variety of

(24) Equation 1 can also be used to approximate the high-temperature section of the $\chi_M T$ curve of compound **3** because both **2b** and **3** (although differing in their supramolecular arrangements) are (locally) somewhat similar in that they contain tetrahedral Co(II) ions linked by pymo bridges.

(25) (a) Rettig, S. J.; Sánchez, V.; Storr, A.; Thompson, R. C.; Trotter, J. *J. Chem. Soc., Dalton Trans.* **2000**, 3931. (b) Rettig, S. J.; Thompson, R. C.; Trotter, J.; Xia, S. *Inorg. Chem.* **1999**, *38*, 1360.

(26) Carlin, R. L. *Magnetochemistry*; Springer-Verlag: Berlin, 1986.

(27) Fernández, I.; Ruiz, R.; Faus, J.; Julve, M.; Lloret, F.; Cano, J.; Ottenwaelder, X.; Journaux, Y.; Muñoz, M. C. *Angew. Chem., Int. Ed.* **2001**, *40*, 3039.

(28) Lloret, F.; De Munno, G.; Julve, M.; Cano, J.; Ruiz, R.; Caneschi, A. *Angew. Chem., Int. Ed.* **1998**, *37*, 135.

(29) Tabares, L. C.; Navarro, J. A. R.; Salas, J. M.; Willermann, M. *Inorg. Chim. Acta* **2001**, *318*, 166.

spectroscopic and magnetic properties of the materials reported. Worth noting is the interesting spin-canted magnetic behavior of **3**, which is related to its acentric crystal structure, resulting from the relative orientations of the ligands bound to tetrahedral metal building blocks, and the spin-polarization effect exerted by the pyrimidine-2-olate ligands acting in the *N,N′-exo*-bidentate-bridging mode. The present contribution substantiates the tremendous importance of coupling different techniques—in the spectroscopic, magnetic, and structural fields—to disclose the chemico-physical properties of a *whole class* of compounds. In this context, the fundamental role of ab initio structure solution from powder diffraction data clearly emerges as the only tool to obtain valuable, *otherwise* inaccessible, crystallographic information in cases in which suitable single crystals are not available.

Acknowledgment. The Italian MIUR and the Chamber of Commerce of Como (N.M., S.G., and A.S.) as well as the Spanish Ministerio de Ciencia y Tecnología and the Junta de Andalucía are acknowledged for funding (E.B., J.A.R.N., J.M.S., and L.T.). E.B. also thanks the Spanish Ministerio de Educación, Cultura y Deporte for a FPU grant. Dr. Luis Lezama from Departamento de Química Inorgánica of the Universidad del País Vasco is acknowledged for acquisition of magnetic data on **3** material.

Supporting Information Available: Tables of crystallographic data for compounds **1** and **2b** (PDF). This material is available free of charge via the Internet at http://pubs.acs.org.

CM030195K